TRANSACTIONS OF THE INSTITUTE OF AVIATION eISSN 2300-5408
No. 1(238), pp. 54-69, Warsaw 2015

INFLUENCE OF ROTOR PARAMETER CHANGES ON HELICOPTER PERFORMANCE AND THE MAIN ROTOR LOAD LEVEL

Jarosław Stanisławski

New Technology Center, Aircraft Design Department, Institute of Aviation, al. Krakowska 110/114, 02-256 Warsaw, Poland, stanjar@ilot.edu.pl

Abstract

Paper presents the results of calculations revealing the influence of changes the main rotor significant parameters like number of blades and rotational speed on helicopter performance and on rotor loads. The level of noise for rotor operated in hover condition is estimated. The rotor loads are defined applying simulation program which includes model of deformable blade. A Runge-Kutta method is used to solve the equations of motion of the elastic blade.

Keywords: helicopter, rotor, performance.

INTRODUCTION

Essential parts of a helicopter structure, which significantly determine its performance, are the main rotor and the level of power developed by engines. The choice of the proper power unit and configuration of the main rotor has an impact on such a helicopter performance like: the maximum flight speed, climbing speed or the level of vibration. The basic features of the main rotor are the number of blades and the speed of the blade tip connected with the rotation speed of the rotor shaft.

An increasing number of rotor blades is one of the methods of improving the helicopter's characteristics. The new rotor with an increased number of blades was applied by Aerospatiale/Eurocopter concern developing the family of a medium helicopter from SA 330 Puma with a four-blade to five-blade EC 725 Caracal version. A similar way of rotorcraft development can be noticed for Hughes/Mc Donnell Douglas. The OH-6A Cayuse helicopter had a four-bladed rotor, an improved version MD500E was equipped with a five-bladed rotor and the newest unmanned version AH-6i Little Bird flies with a six-bladed rotor. A successful example of improving the features of an old helicopter is modernization of Sikorsky S-55 model including an installation of a turbine power unit and applying a new five-bladed rotor with a reduced blade tip speed [1]. The improved version of the helicopter dubbed Whisper Jet obtained a very low noise level. The helicopter was allowed for viewing flights over the Grand Canyon National Park.

The following analysis concerns the possibilities of changing the helicopter operating features by applying the increased, from three to six, number of rotor blades and reducing the rotor blade tip speed ranging from high value 220 m/s to a lower one of 160 m/s.

For the simulation calculations two models of the main rotor were used. In a simplified model, the rotor was treated as a disk area with an average value of induced speed and aerodynamic coefficients. By applying a simplified rotor model the following parameters were defined as a function of flight speed: the helicopter equilibrium conditions, the rotor thrust components and the power required to drive the main and tail rotors for a different number of rotor blades and a different blade tip speed. The more precise model of the rotor comprises deflections of individual blades. The blade is represented by a set of lumped masses and sections of an elastic axis allowing for torsion and bending in-plane and out-of-plane deformations. In accordance with the Galerkin method, the blade motion is treated as a resultant combination of a considered blade torsion and bending eigen modes. Equations of motion of the elastic blade are solved by using the Runge-Kutta method. Defining the distribution of blade deflections and loads on the rotor disk enable calculation of resultant loads of the rotor hub and the rotor control system [2], [3].

HELICOPTER PERFORMANCE

The simulation calculations for possibilities of performance changes were performed for the data of hypothetical helicopter with the total mass 1,000 kg and the main rotor radius 3.75 m. The calculations comprise the power required for driving a three-bladed main rotor (Fig. 1) and a six-bladed rotor (Fig. 2) with changing the blade tip speed from 160 m/s to 220 m/s. Both versions of the rotor consist of blades of the same geometry. For the considered variants of the main rotor values of the power required to drive the tail rotor consisting of five blades (Fig. 3 and Fig. 4) were also determined. For each case, a combination of number of the main rotor blades and a blade tip speed, the tail rotor thrust for equilibrium condition was calculated (Fig. 5 and Fig. 6).

Analyzing the plots of the main rotor required power in Fig. 1, it can be noticed that for a three-bladed rotor in the range of flight speed below 130 km/h the lower values of the required power occur for the blade tip speed scope between 180 m/s and 190 m/s. The case of a lesser blade tip speed of 160 m/s, beneficial for a low noise level, requires bigger power in hover conditions. For a large flight speed of about 200 km/h lesser values of the rotor required power occur at the blade tip speed of 210-220 m/s range. At flight speed close to 200 km/h for an advancing blade, the effects of compressibility are not significant enough to cause additional growth of the power required. At the relatively high blade tip speed of 220 m/s the local angles of attack are lesser compared to the case of rotor blades with tip speed of 160 m/s which can explain the biggest value of the rotor required power in the case of the tip speed of 160 m/s.

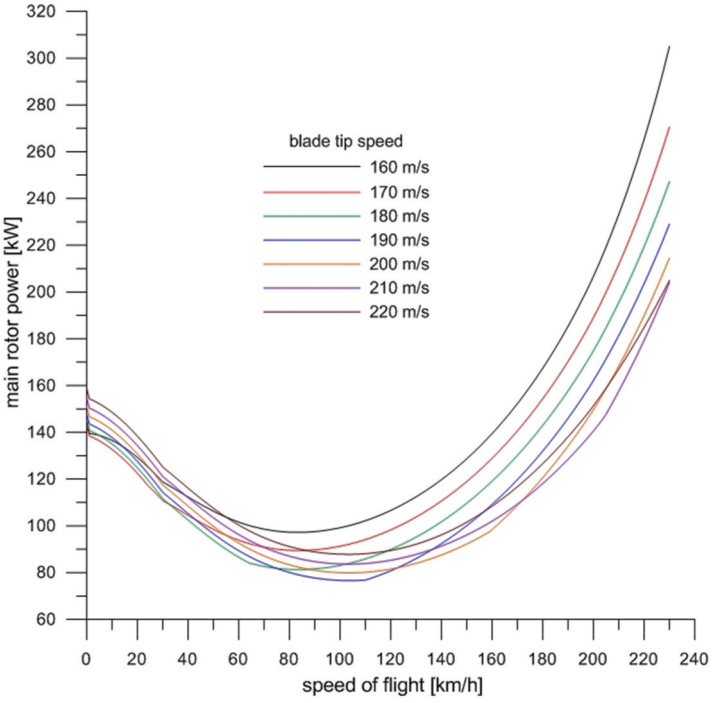

Fig. 1. Power required to drive the main rotor depending on flight speed and on rotor blade tip speed, helicopter mass 1,000 kg, three-bladed rotor [J. Stanisławski, 2014]

In the case of a six-bladed rotor (Fig. 2) small values of attack angles of the blade cross-sections cause the lowest level of required power, at the lowest blade tip speed of 160 m/s. Respectively, the lower power of the main rotor requires the lower power to drive the tail rotor. For a six-bladed main rotor the power of a five-bladed tail rotor with the tail blade tip speed of 152 m/s (bonded with the main rotor blade tip V_{tip} = 160 m/s) is lower than 4 kW even for a flight speed condition V = 240 km/h (Fig. 4).

In Fig. 7÷Fig. 9 are presented the effects on required power for increasing the number of rotor blades from three to six, for two values of tip speed of 160 m/s (Fig. 7) and of 220 m/s (Fig. 8). Increasing the number of rotor blades enables to preserve the low level of the rotor required (150-180 kW) even for a slow blade tip speed of 160 m/s (Fig. 7). In Fig. 9 is shown the comparison of changes the rotor required power as a function of the flight speed for extreme cases of the blade tip speed and the numbers of blades. As it can be seen, the lowest level of the rotor power is reached for the case of a slow rotating six-bladed rotor.

Fig. 10 presents the estimation of noise generated by a helicopter in hover at 150 m above the ground. According to the formula by Davidson and Hargest [4], the sound pressure level beneath the rotor hub can be as follows:

$$SPL150 = 10\log[(\Omega R)^6 A_b (c_t / \sigma)^2] - 36.7\ [dB]$$

where:

- thrust coefficient

$$c_t = \frac{T}{\rho \cdot \pi R^2 \cdot (\Omega \cdot R)^2}$$

- T – rotor thrust, [N]
- ρ – air density, [kg/m^3]
- R – rotor radius, [m]
- ΩR – blade tip speed, [m/s]
- A_b – summary area of rotor blades, [m^2]
- σ – ratio of blade area to rotor disk area, σ = k b/π/R
- k – number of blades,
- b – blade chord, [m]

The lowest sound level equal 79 dB is generated by a six-bladed rotor for the lowest considered blade tip speed of 160 m/s.

The effects of possibility continuous regulation of the rotor speed can be useful for tracking optimal or economic flight conditions with changes of the helicopter mass due to fuel consumption. In Fig. 11 are shown the limits of change of the blade tip speed as a function of flight time in the optimal conditions. Fig. 12 and Fig. 13 present changes of a blade collective pitch for three and six-bladed rotors. The blade collective pitch is given for the same cases as for the calculations of the rotor required power shown in Fig. 1 and Fig. 2. The change limits of the blade pitch for extreme cases are compared in Fig. 14. The lowest values of the blade collective pitch are for the case of a six-bladed rotor with the highest tip speed. Similarly, the term of equilibrium are preserved at a lower pitch angle of tail rotor blades for high tail rotor blade tip speed (Fig. 15).

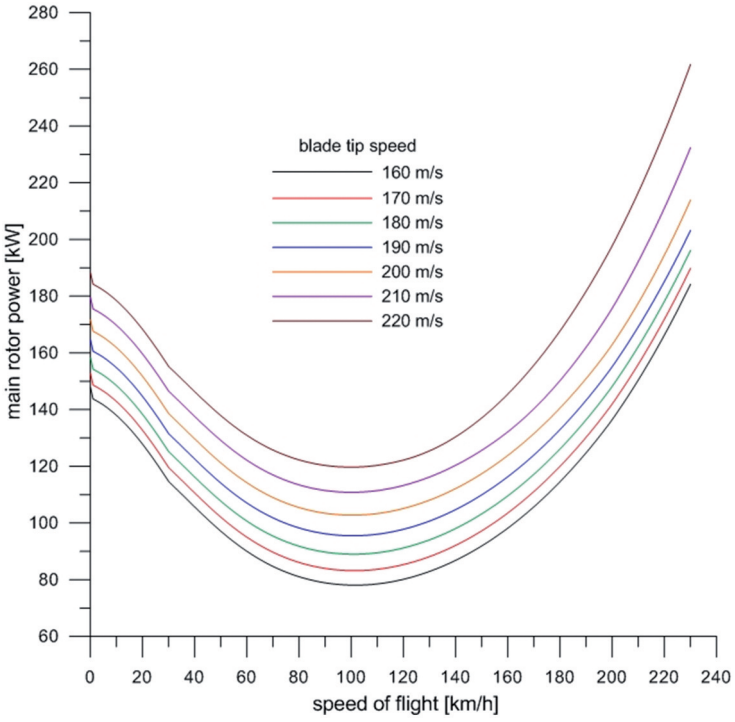

Fig. 2. Power required to drive the main rotor depending on flight speed and on rotor blade tip speed, helicopter mass 1,000 kg, six-bladed rotor [J. Stanisławski, 2014]

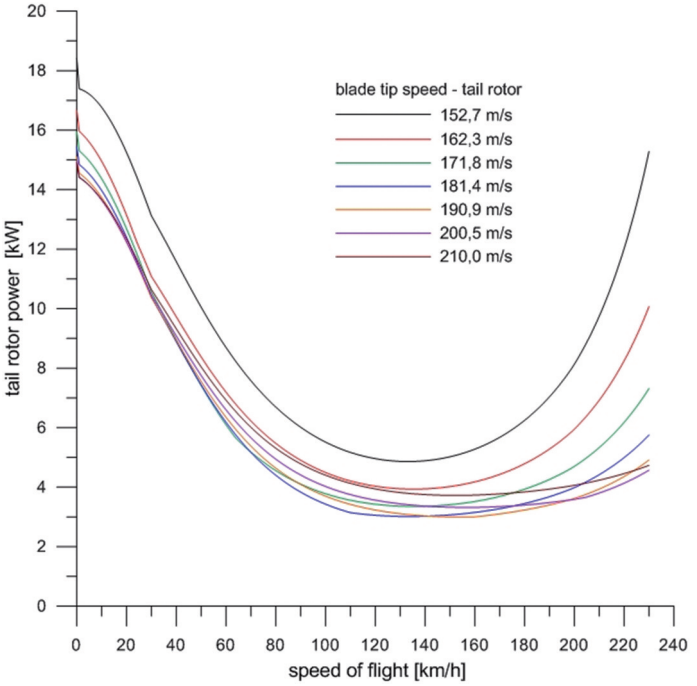

Fig. 3. Power required to drive tail rotor due to flight speed and blade tip speed helicopter mass 1,000 kg, five-bladed tail rotor. The case for three-bladed main rotor [J. Stanisławski, 2014]

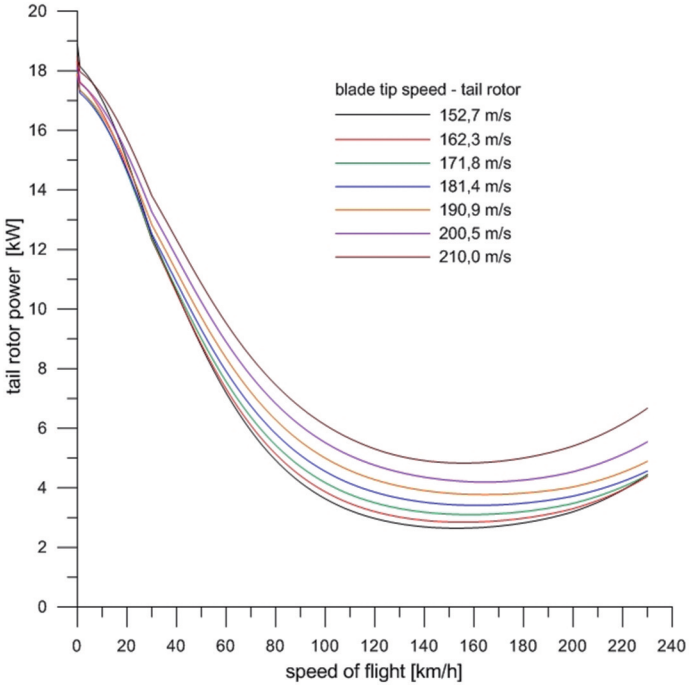

Fig. 4. Power required to drive tail rotor due to flight speed and blade tip speed, helicopter mass 1,000 kg, five-bladed tail rotor. The case for six-bladed main rotor [J. Stanisławski, 2014]

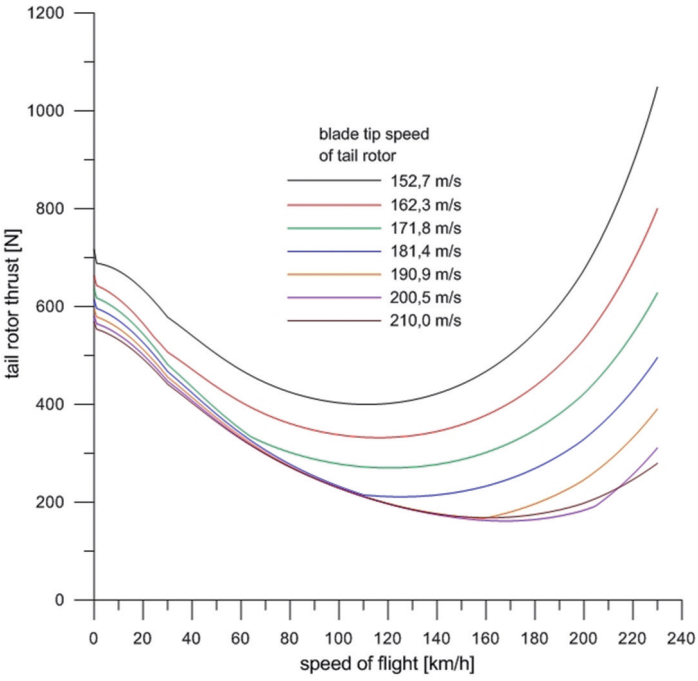

Fig. 5. Required for equilibrium the tail rotor thrust due to flight speed and blade tip speed of tail rotor, helicopter mass 1,000 kg, five-bladed tail rotor. The case for three-bladed main rotor [J. Stanisławski, 2014]

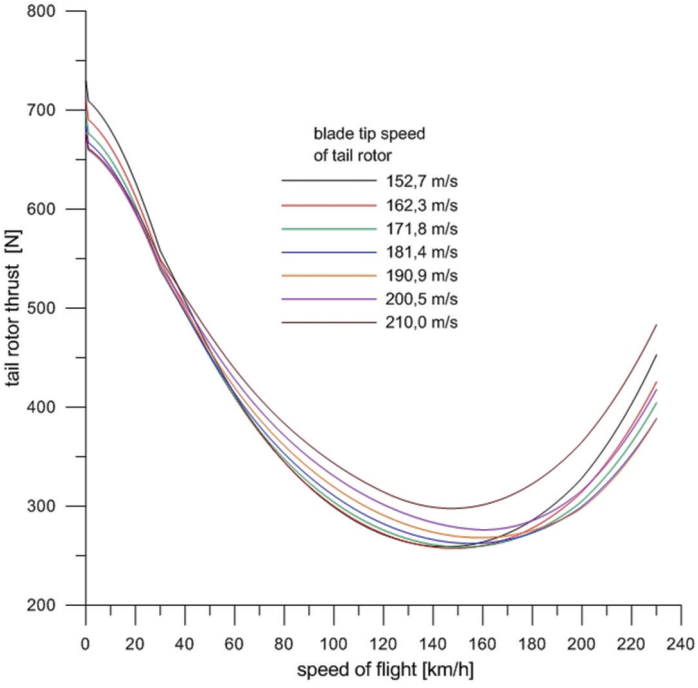

Fig. 6. Required for equilibrium the tail rotor thrust due to flight speed and blade tip speed of tail rotor, helicopter mass 1,000 kg, five-bladed tail rotor. The case for six-bladed main rotor [J. Stanisławski, 2014]

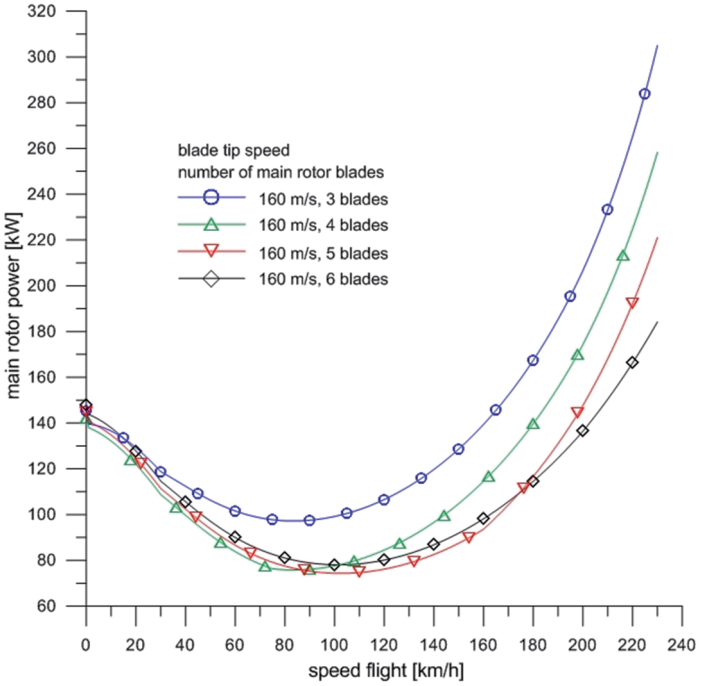

Fig. 7. Power required to drive the main rotor depending on flight speed and on number of main rotor blades, helicopter mass 1,000 kg. The cases for blade tip speed $V_{\Omega R}$ = 160 m/s [J. Stanisławski, 2014]

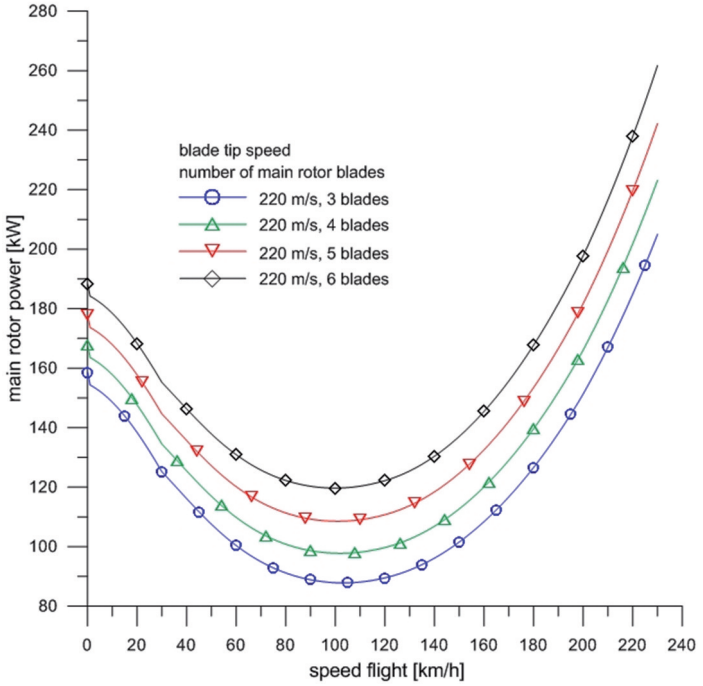

Fig. 8. Power required to drive the main rotor depending on flight speed and on number of main rotor blades, helicopter mass 1,000 kg. The cases for blade tip speed $V_{\Omega R}$ = 220 m/s [J. Stanisławski, 2014]

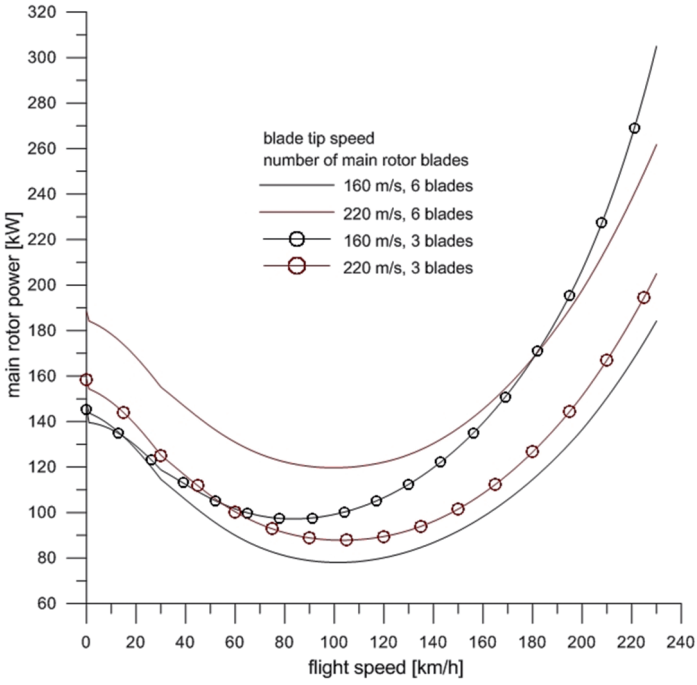

Fig. 9. Power required to drive the main rotor depending on flight speed and on rotor blade tip speed, helicopter mass 1,000 kg. The cases for three-bladed rotor and six-bladed rotor [J. Stanisławski, 2014]

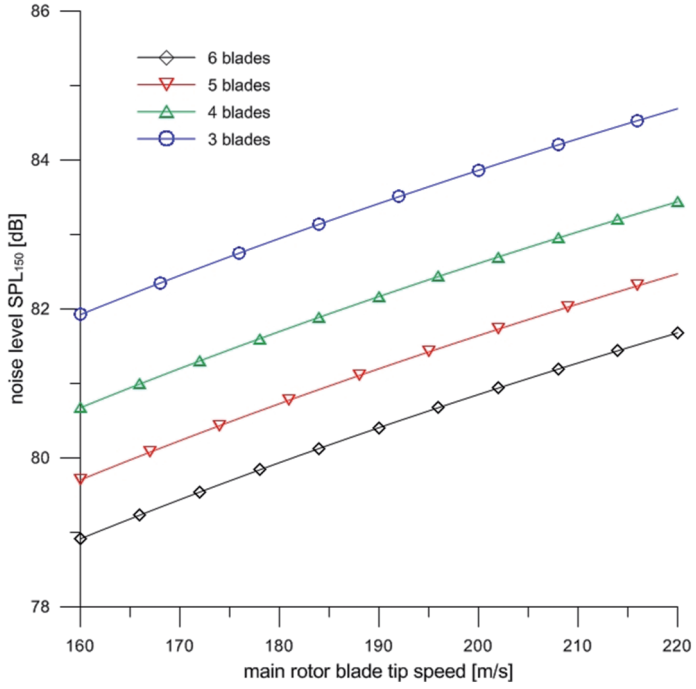

Fig. 10. Main rotor noise level generated in hover condition due to blade tip speed and number of blades, helicopter mass 1,000 kg [J. Stanisławski, 2014]

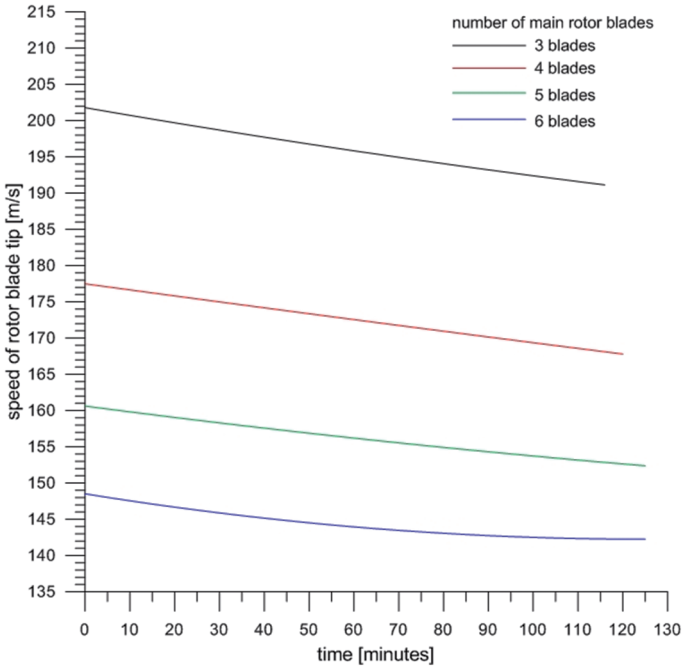

Fig. 11. Changes of rotor blade tip speed during flight in optimal conditions taking into account reduction of helicopter mass due to fuel consumption. The cases for helicopter total mass 1,000 kg, the same fuel mass m_{fuel} = 100 kg and different number of main rotor blades [J. Stanisławski, 2014]

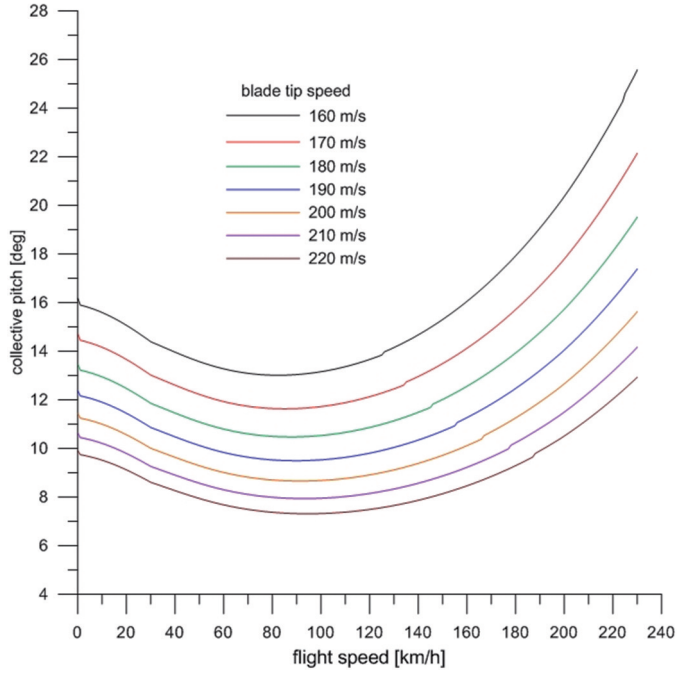

Fig. 12. Collective pitch of the main rotor blades as function of flight speed and blade tip speed. The case for three-bladed rotor and helicopter mass 1,000 kg [J. Stanisławski, 2014]

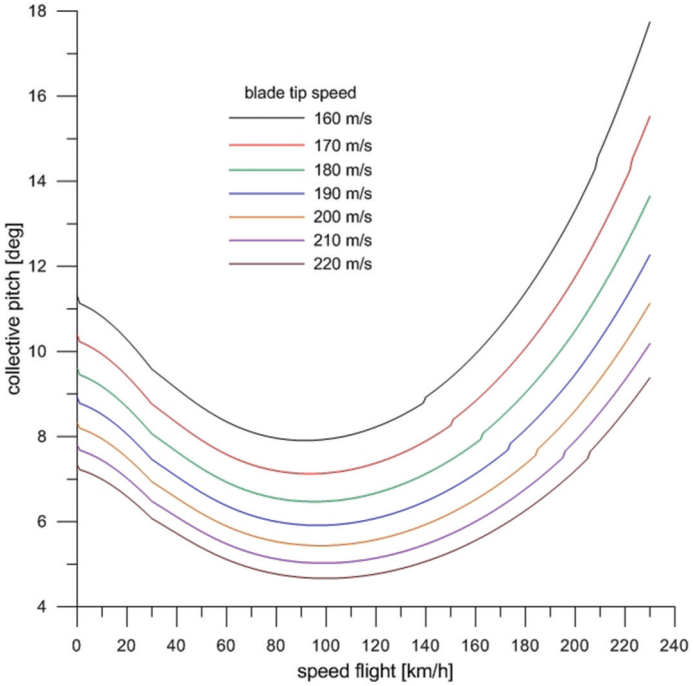

Fig. 13. Collective pitch of the main rotor blades as function of flight speed and blade tip speed. The case for six-bladed rotor and helicopter mass 1,000 kg [J. Stanisławski, 2014]

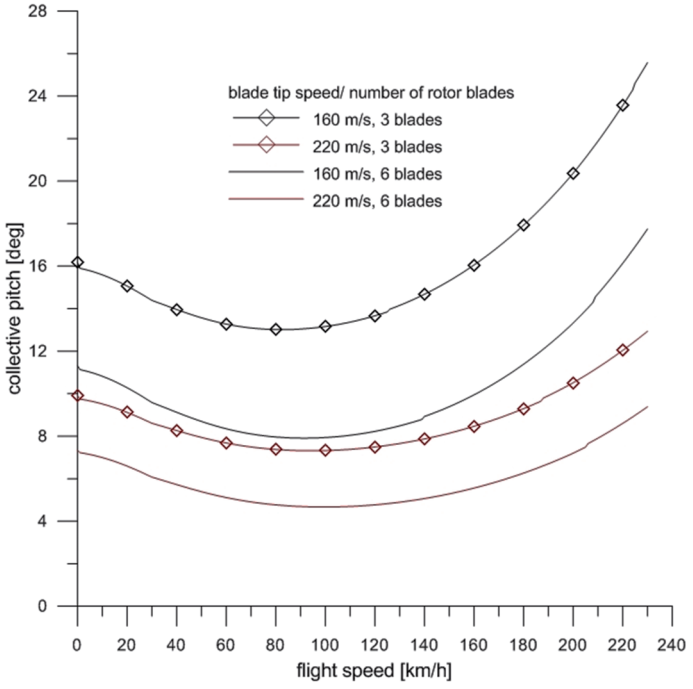

Fig. 14. Comparison of change range of the main rotor blades collective pitch due to flight speed and blade tip speed, case for helicopter mass 1,000 kg with three-bladed or six-bladed main rotor versions [J. Stanisławski, 2014]

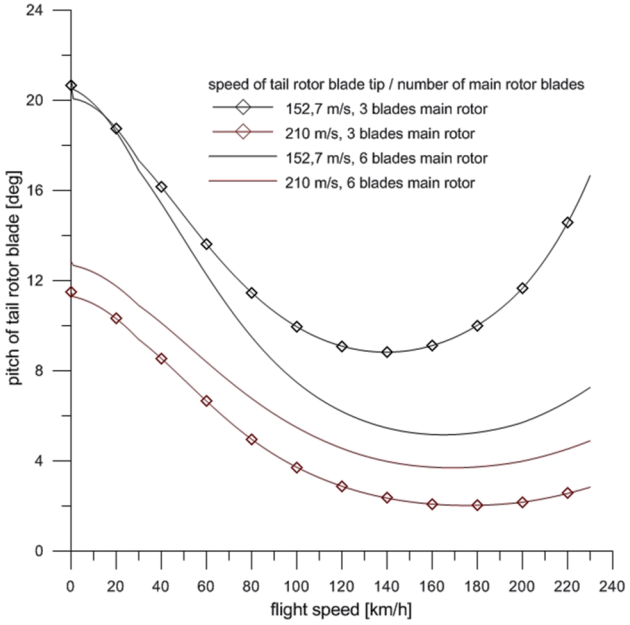

Fig. 15. Comparison of change range of the tail rotor blades pitch due to flight speed and blade tip speed. The cases for helicopter mass 1,000 kg with three-bladed or six-bladed main rotor versions and five-bladed tail rotor [J. Stanisławski, 2014]

ROTOR LOADS

Applying for simulating calculations a more precise model of elastic rotor blades allows to define limits of variable blade loads as function of azimuth position on rotor disk and estimate the influence of blades number on amplitude and frequency of rotor loads. The simulating calculations for each selected case of the blade number and the blade tip speed were executed for time limits corresponding to the twelve revolutions of rotor. Plots show the results for the last two revolution of the rotor, when the effects of start condition were diminished.

In Fig. 16÷Fig. 23 are presented the results for selected cases of level flight speed of 200 km/h with applied blade tip speed of 160 m/s. For variants of rotors with three, four, five and six blades are shown the plots of rotor required power (Fig. 16) and changes of rotor thrust (Fig. 17) during the rotor revolution. The lowest oscillations occur for a six-bladed rotor. Large changes of power and thrust for three-bladed rotor are connected with an appearance of a flow separation zone at the tip and middle cross-sections of blades (Fig. 22). Increasing the number of blades allows to reduce collective and cyclic pitch for providing the generation of the proper value of rotor thrust and reducing the separation flow zone, which is shown in Fig. 23 for four-bladed rotor case. An increased blade number gives a higher frequency of power and thrust of the main rotor with a significant amplitude reduction, even for the case of five-bladed and six-bladed rotor where, there was no separation flow on the tip cross-sections of the blade. The evident effects of separation flow can be noticed as a lower mean value of the rotor thrust for the case of a three-bladed rotor (Fig. 17). The influence of separation zone for a three-bladed and four-bladed rotor is observed in plots of control system loads: control pitch moment for a single blade (Fig. 18) and a control force of a collective pitch for all blades (Fig. 19). For the loads of a rotor control system, a higher number of blades causes increment of the mean value of the control force of collective pitch with simultaneous reduction of amplitude (Fig. 19). Changes of the attack angle at the tip cross-sections of the rotor blade as a function of the azimuth position are shown in Fig. 20. Comparing the plots for three-bladed and six-bladed rotor can

be noticed the 10° reduction of the maximum value of attack angles. The minimum of attack angles existing for advancing blade position at azimuth 90° preserve nearly the same level equal about -2°. The effects of separation flow is also clearly seen in plots of torsion deflections of the blade tip (Fig. 21). For a three-bladed rotor large changes of torsion blade loads cause oscillations corresponding to blade torsion eigen mode even in azimuth zone without a separation flow. The harmful influence of a separation disappears with an increasing number of rotor blades, which enables to generate a higher value of thrust with preserved angles of attack below critical values.

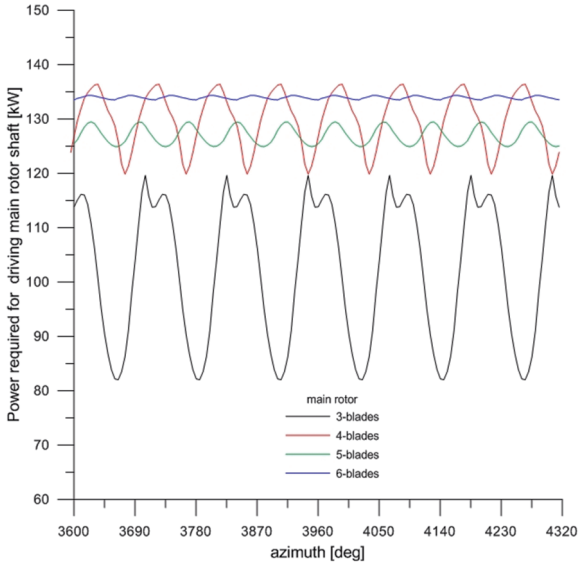

Fig. 16. Power required for driving the main rotor shaft in level flight condition at speed V = 200 km/h, rotor blade tip speed $V_{\Omega R}$ = 160 m/s, main rotor versions: three, four, five and six blades [J. Stanisławski, 2014]

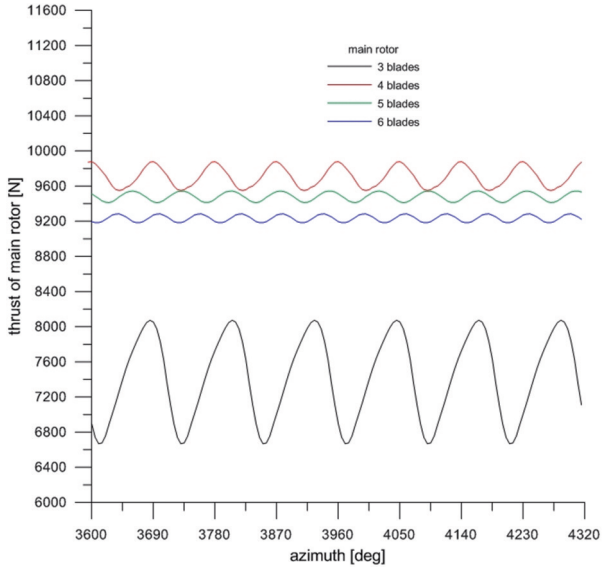

Fig. 17. Main rotor thrust in level flight condition at speed V = 200 km/h, main rotor blade tip speed $V_{\Omega R}$ = 160 m/s, rotor variants: three, four, five, six blades [J. Stanisławski, 2014]

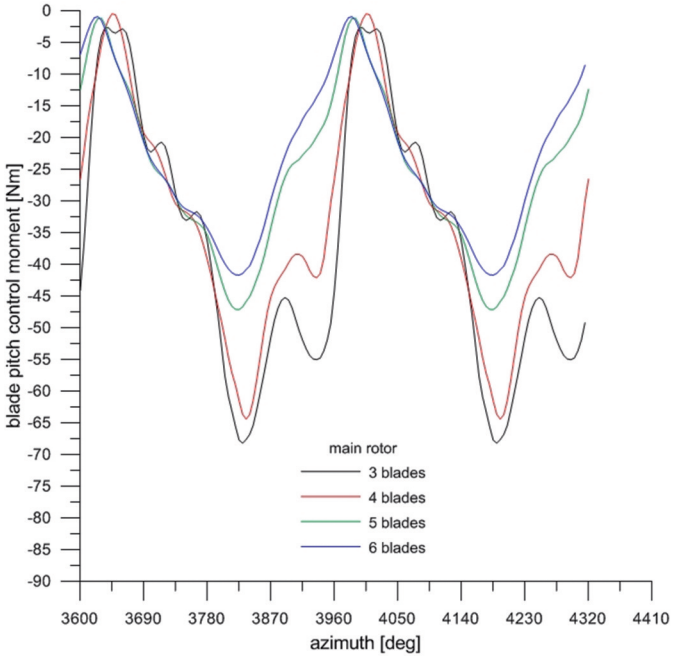

Fig. 18. Changes of pitch control moment of main rotor blade as function of azimuth position in level flight conditions at speed v = 200 km/h, main rotor blade tip speed $V_{\Omega R}$ = 160 m/s, rotor variants: three, four, five and six blades, simulation solution for 11th and 12th rotor revolution [J. Stanisławski, 2014]

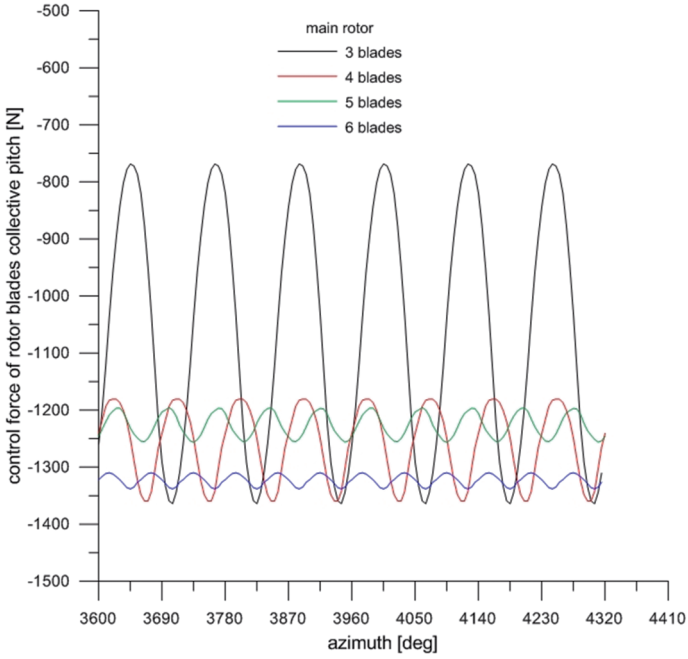

Fig. 19. Control force of collective pitch of all main rotor blades in level flight conditions at speed v = 200 km/h, main rotor blade tip speed $V_{\Omega R}$ = 160 m/s, rotor variants: three, four, five and six blades, simulation solution for 11th and 12th rotor revolution [J. Stanisławski, 2014]

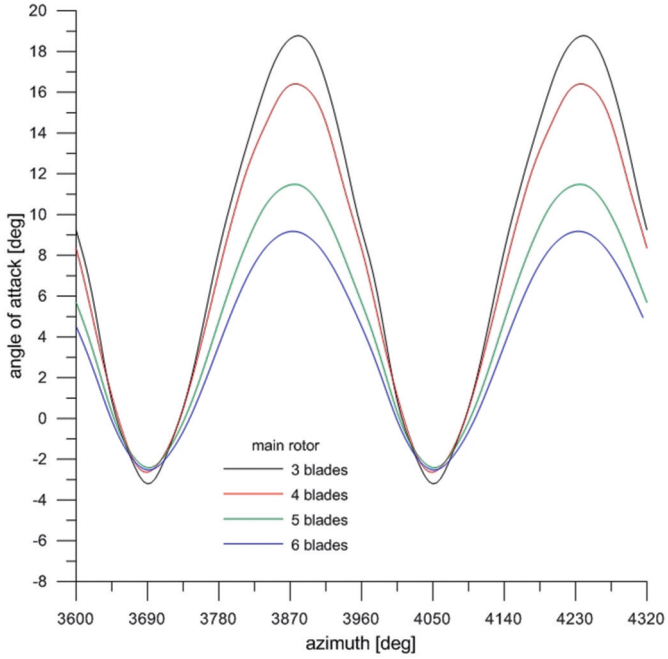

Fig. 20. Angle of attack at tip of rotor blade as function of azimuth position in level flight conditions at speed V = 200 km/h, main rotor blade tip speed $V_{\Omega R}$ = 160m/s, rotor variants: three, four, five and six blades, simulation solution for 11th and 12th rotor revolution [J. Stanisławski, 2014]

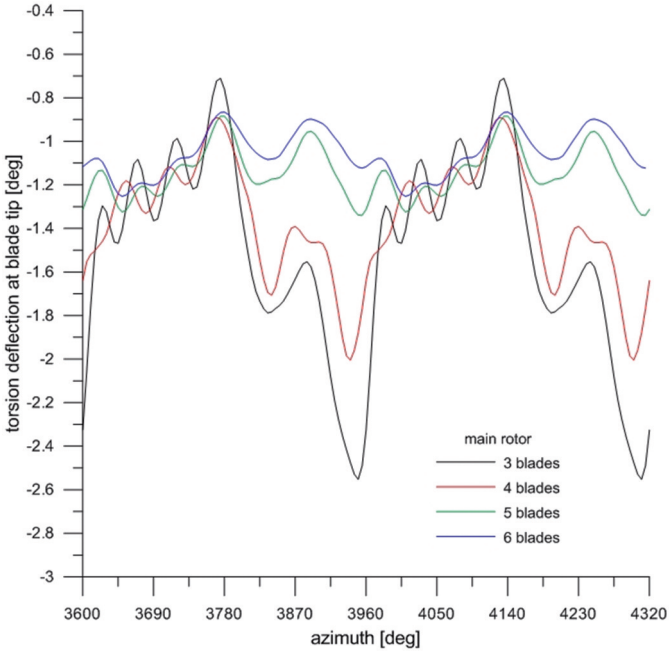

Fig. 21. Torsion deflection of rotor blade at tip section as function of blade azimuth position in level flight conditions at speed v = 200 km/h, main rotor blade tip speed $V_{\Omega R}$ = 160 m/s, rotor variants: three, four, five and six blades, simulation solution for 11th and 12th rotor revolution [J. Stanisławski, 2014]

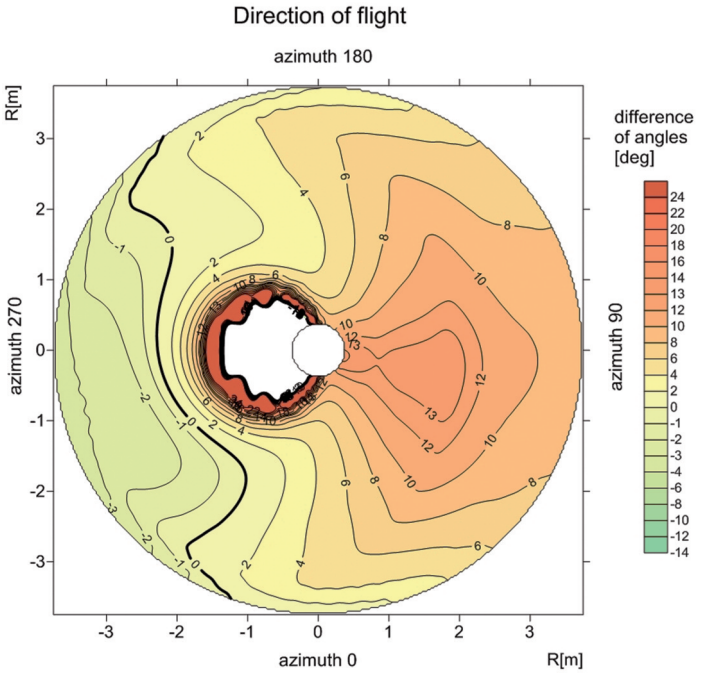

Fig. 22. Rotor disk distribution of difference of critical and local attack angles of blade cross-sections in level flight at speed 200 km/h. The case for three-bladed rotor with blade tip speed 160 m/s [J. Stanisławski, 2014]

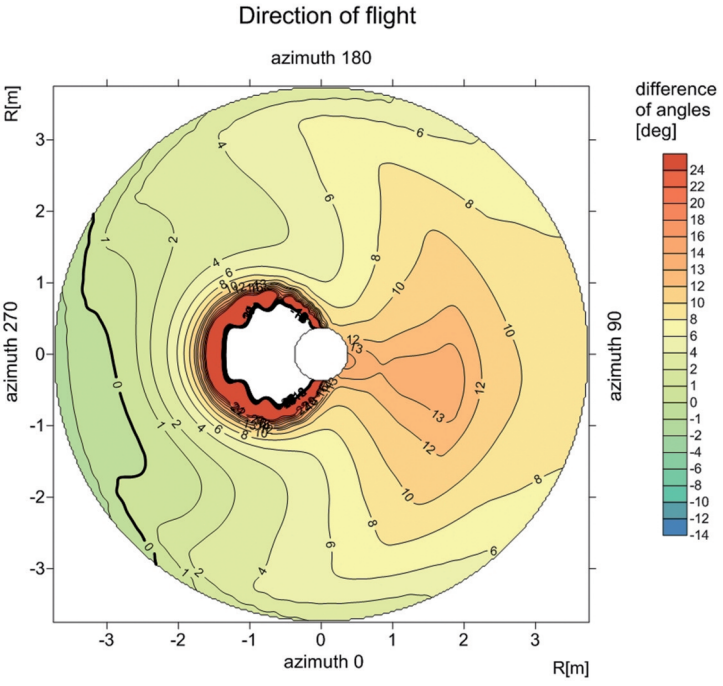

Fig. 23. Rotor disk distribution of difference of critical and local attack angles of blade cross-sections in level flight at speed 200 km/h. The case for four-bladed rotor with blade tip speed 160 m/s [J. Stanisławski, 2014]

CONCLUSIONS

The simulated calculations indicate advantages of applying the main rotor with an increased number of blades, a reduced blade tip speed and introduced a possibility of the rotor speed control within wider limits for adaptation to changing optimal or economic flight conditions.

A high number of rotor blades enables flow conditions of blade cross-sections without a separation zone, which provides a lower amplitude of variable loads of the rotor and the whole structure of the helicopter.

An additional low blade tip speed decreases the sound pressure level generated by the helicopter rotor.

REFERENCES

[1] Flight International. 1-7 February 2000. p. 29.
[2] Stanisławski, J. (2012). Obliczenia obciążeń śmigłowca ILX-27, Institute of Aviation, internal report ILX27/0001/BP2/2012, Warszawa, (in Polish).
[3] Stanisławski, J. (2013). Porównanie wyników pomiarów oraz symulacji obliczeniowych pracy śmigłowca ILX-27, Institute of Aviation, internal report ILX27/0014/BP2/2013, Warszawa, (in Polish).
[4] Johnson, W. (2013). *Rotorcraft Aeromechanics*, New York, Cambridge University Press.

WPŁYW ZMIAN PARAMETRÓW WIRNIKA NA OSIĄGI ŚMIGŁOWCA ORAZ POZIOM OBCIĄŻEŃ WIRNIKA

Streszczenie

Przedstawiono efekty zmian podstawowych parametrów wirnika nośnego, jak liczba łopat i prędkość obrotowa wirnika na osiągi śmigłowca oraz na obciążenia wirnika nośnego. Zamieszczono przybliżoną ocenę wpływu zmian własności wirnika na poziom generowanego hałasu. Obciążenia wirnika wyznaczano metodą symulacyjną przy wykorzystaniu programu uwzględniającego model odkształcalnej łopaty. Do rozwiązania równań ruchu elastycznej łopaty zastosowano metodę Runge-Kutta.

Słowa kluczowe: śmigłowiec, wirnik, osiągi.